Nonlinear Analysis: Modelling and Control, Vol. 26, No. 2, 207–226
https://doi.org/10.15388/namc.2021.26.21203

Vilnius University Press

Mittag–Leffler synchronization for impulsive fractional-order bidirectional associative memory neural networks via optimal linear feedback control*

Jiazhe Lin[a], **Rui Xu**[b,1], **Liangchen Li**[c]

[a]Computational Aerodynamics Institute,
China Aerodynamics Research and Development Center,
Mianyang 621000, China

[b]Complex Systems Research Center, Shanxi University,
Taiyuan 030006, China
xurui@sxu.edu.cn

[c]Institute of Applied Mathematics, Army Engineering University,
Shijiazhuang 050003, China

Received: December 19, 2019 / **Revised:** November 26, 2020 / **Published online:** March 1, 2021

Abstract. In this paper, we are concerned with the synchronization scheme for fractional-order bidirectional associative memory (BAM) neural networks, where both synaptic transmission delay and impulsive effect are considered. By constructing Lyapunov functional, sufficient conditions are established to ensure the Mittag–Leffler synchronization. Based on Pontryagin's maximum principle with delay, time-dependent control gains are obtained, which minimize the accumulative errors within the limitation of actuator saturation during the Mittag–Leffler synchronization. Numerical simulations are carried out to illustrate the feasibility and effectiveness of theoretical results with the help of the modified predictor-corrector algorithm and the forward-backward sweep method.

Keywords: Mittag–Leffler synchronization, BAM neural network, fractional derivative, impulsive effect, optimal control, actuator saturation.

1 Introduction

Forward and backward information flow is introduced in neural networks to produce two-way associative search for stored stimulus-response associations. Above mentioned neural network is usually referred to as BAM neural network, which behaves as a two-layer hierarchy of symmetrically connected neurons [12]. In the past few decades, BAM neural networks as well as their various generalizations have attracted the attention of

*This research was supported the National Natural Science Foundation of China (Nos. 11871316, 11801340, 11371368) and the Natural Science Foundation of Shanxi Province (Nos. 201801D121006, 201801D221007).

[1]Corresponding author.

many researchers due to their potential applications in parallel computation, associative memory, nonlinear optimization problem and so on [29, 33]. BAM neural networks are originally proposed by Kosko [12], which are described by the following system:

$$\begin{aligned}\frac{\mathrm{d}x_i(t)}{\mathrm{d}t} &= -c_i^{(1)}x_i(t) + \sum_{j=1}^{m} a_{ji}^{(1)} f_j\big(y_j(t)\big) + I_i^{(1)}, \quad i = 1, 2, \ldots, n,\\ \frac{\mathrm{d}y_j(t)}{\mathrm{d}t} &= -c_j^{(2)}y_j(t) + \sum_{i=1}^{n} a_{ij}^{(2)} g_i\big(x_i(t)\big) + I_j^{(2)}, \quad j = 1, 2, \ldots, m,\end{aligned} \tag{1}$$

which consists of two layers $U = \{x_1, x_2, \ldots, x_n\}$ and $V = \{y_1, y_2, \ldots, y_m\}$. $x_i(t)$ and $y_j(t)$ denote the membrane voltages of ith neuron in the U-layer and the membrane voltages of jth neuron in the V-layer, respectively; $c_i^{(1)}$ and $c_j^{(2)}$ are the rates with which the ith or jth unit resets its potential to the resting state in isolation when disconnected from the network and external inputs; $a_{ji}^{(1)}$ and $a_{ij}^{(2)}$ are the connection weights through the neurons. On the U-layer, the neurons whose states are denoted by $x_i(t)$ receive the inputs $I_i^{(1)}$ and the inputs outputted by those neurons in the V-layer via activation functions $f_j(\cdot)$, while on the V-layer, the neurons whose states are denoted by $y_j(t)$ receive the inputs $I_j^{(2)}$ and the inputs outputted by those neurons in the U-layer via activation functions $g_i(\cdot)$.

In system (1), it is assumed that neurons respond synchronously to signals. Due to the finite speed of signal transmission and amplifiers switching, time delay inevitably exists in neural networks, which is known as synaptic transmission delay. Usually, time delay has a great influence on the dynamical behaviors and synchronization control of neural networks. For example, Hu et al. [10] investigated the global synchronization criteria for time-invariant uncertainty fractional-order neural networks, where the synchronization criteria include time delay information.

Besides, traditional neural networks are mainly established based on integer-order derivatives, which can be described by classical ordinary differential equations. In recent years, experimental research indicates that fraction-order derivatives provide an excellent tool for the description of memory and hereditary properties of various materials and processes [2, 18]. Generally speaking, plenty of practical objects can be described clearly by the fractional differential equations, due to their more degrees of freedom and infinite memory. Thus, the research of fractional neural networks has gained much attention and some valuable results have been referred to [17, 27].

The synchronization of dynamical systems corresponds to a dynamical process where the behavior of different dynamical systems tends to be consistent by coupling effect or external control [32]. There have been several works on synchronization problems with respect to the fractional-order neural networks via various control approaches such as impulsive control [35], linear feedback control [26], sliding model control [6], event-triggered control [22] and so on. Ye et al. [32] established sufficient conditions to ensure the global Mittag–Leffler synchronization based on the delayed-feedback control strategy. Ding et al. [9] studied the synchronization for a class of fractional-order BAM neural networks with time delays and discontinuous activation functions, where the state feedback

and impulsive controllers are designed to ensure the Mittag–Leffler synchronization, respectively.

However, the control gains of various controllers in the above-mentioned researches are set as constants based on experience, which are not optimal. Furthermore, actuator saturation is one of the most important non-smooth input nonlinearities in the control system. In general, most of the practical network applications contain a huge number of actuators and their physical capacity is quite limited. It is difficult to deliver arbitrarily large signals through real actuators [23, 28], namely, the practical physical actuators can only generate bounded amplitude signals, where the control system will provide poor performance or even become unstable [24, 30]. Hence, during the Mittag–Leffler synchronization, it is of great practical significance to realize optimal synchronization control which minimizes the accumulative errors within the limitation of actuator saturation.

In this paper, we mainly focus on finding time-dependent control gains of optimal linear feedback controllers. In addition, the states of artificial neural networks are often subject to instantaneous perturbations and experience abrupt changes at certain instants, which may be caused by switching phenomenon, frequency change or other sudden noise, that exhibit impulsive effects. Thus, it is necessary to take the impulsive effects into account [13, 19]. To this end, we consider the following impulsive fractional-order BAM neural network with synaptic transmission delay:

$$\begin{aligned}
&{}_0^C D_t^q x_i(t) = -c_i^{(1)} x_i(t) + \sum_{j=1}^{m} a_{ji}^{(1)} f_j\big(y_j(t)\big) \\
&\qquad\qquad + \sum_{j=1}^{m} b_{ji}^{(1)} f_j\big(y_j\big(t-\eta_{ji}(t)\big)\big) + I_i^{(1)}, \quad t \neq t_k, \\
&\Delta x_i(t) = \gamma_k^{(1)}\big(x_i(t)\big), \quad t = t_k, \quad i = 1, 2, \ldots, n,\ k = 1, 2, \ldots, \\
&{}_0^C D_t^q y_j(t) = -c_j^{(2)} y_j(t) + \sum_{i=1}^{n} a_{ij}^{(2)} g_i\big(x_i(t)\big) \\
&\qquad\qquad + \sum_{i=1}^{n} b_{ij}^{(2)} g_i\big(x_i\big(t-\sigma_{ij}(t)\big)\big) + I_j^{(2)}, \quad t \neq t_k, \\
&\Delta y_j(t) = \gamma_k^{(2)}\big(y_j(t)\big), \quad t = t_k, \quad j = 1, 2, \ldots, m,\ k = 1, 2, \ldots .
\end{aligned} \tag{2}$$

${}_0^C D_t^q$ denotes Caputo-type fractional derivative of order q with $0 < q < 1$; $a_{ji}^{(1)}$, $b_{ji}^{(1)}$, $a_{ij}^{(2)}$ and $b_{ij}^{(2)}$ are all the connection weights through the neurons; $\eta_{ji}(t)$ and $\sigma_{ij}(t)$ are synaptic transmission delays.

This paper is organized as follows. In the next section, some necessary assumptions, definitions, and lemmas are listed. Then we investigate the Mittag–Leffler synchronization scheme for system (2). In Section 3, we aim to find optimal linear feedback controllers by Pontryagin's maximum principle with delay. In Section 4, numerical simulations illustrate the analytical predictions obtained in Sections 2 and 3. The paper ends with a conclusion in Section 5.

2 Mittag–Leffler synchronization conditions via linear control

2.1 Preliminaries

Throughout this paper, the following assumptions hold.

(H1) Activation functions $f_i(\cdot)$ and $g_j(\cdot)$ are Lipschitz continuous, namely, there exist positive constants $L_j^f, L_i^g \in \mathbb{R}^+$ such that

$$\begin{aligned} &\big|f_j(y_1) - f_j(y_2)\big| \leqslant L_j^f |y_1 - y_2|, \quad j = 1, 2, \dots, m, \ \forall y_1, y_2 \in \mathbb{R}, \\ &\big|g_i(x_1) - g_i(x_2)\big| \leqslant L_i^g |x_1 - x_2|, \quad i = 1, 2, \dots, n, \ \forall x_1, x_2 \in \mathbb{R}. \end{aligned}$$

(H2) The impulsive operators $\gamma_k^{(1)}$ and $\gamma_k^{(2)}$ satisfy

$$\begin{aligned} &\gamma_k^{(1)}\big(x_i(t_k)\big) = -\lambda_{ik}^{(1)} x_i(t_k), \qquad i = 1, 2, \dots, n, \ k = 1, 2, \dots, \\ &\gamma_k^{(2)}\big(y_j(t_k)\big) = -\lambda_{jk}^{(2)} y_j(t_k), \qquad j = 1, 2, \dots, m, \ k = 1, 2, \dots, \end{aligned}$$

where $\lambda_{ik}^{(1)}, \lambda_{jk}^{(2)} \in (0, 2)$.

(H3) Time-varying delays, including $\eta_{ji}(t)$ and $\sigma_{ij}(t)$, are continuous and bounded on $\mathbb{R}^+$. Thus, there exists a positive constant τ such that $\eta_{ji}(t), \sigma_{ij}(t) \in [0, \tau]$.

(H4) Moreover, impulsive moments $\{t_k | k = 1, 2, \dots\}$ satisfy $0 = t_0 < t_1 < t_2 < \cdots < t_k < \cdots$, $t_k \to +\infty$ as $k \to +\infty$, and

$$\begin{aligned} &x_i(t_k^+) = x_i(t_k) + \gamma_k^{(1)}(x_i(t_k)), \quad x_i(t_k^-) = x_i(t_k), \ i = 1, 2, \dots, n, \\ &y_j(t_k^+) = y_j(t_k) + \gamma_k^{(2)}(y_j(t_k)), \quad y_j(t_k^-) = y_j(t_k), \ j = 1, 2, \dots, m, \end{aligned} \tag{3}$$

in which $x_i(t_k^+)$ and $x_i(t_k^-)$ represent the right and left limits of $x_i(t)$ at $t = t_k$, respectively.

Define a function space $\mathcal{X}(\mathbb{R}, \mathbb{R}) = \{f : \mathbb{R} \to \mathbb{R}$: $f(t)$ is continuous, except for some points $t_k \in \mathbb{R}$ at which $f(t_k^-)$ and $f(t_k^+)$ exist and $f(t_k^-) = f(t_k)\}$. Thus, the initial condition associated with system (2) can be expressed as

$$\begin{aligned} &x_i(t) = \varphi_i(t), \quad t \in [-\tau, 0], \qquad x_i\big(t_0^+\big) = \varphi_i(0), \\ &y_j(t) = \phi_j(t), \quad t \in [-\tau, 0], \qquad y_i\big(t_0^+\big) = \phi_j(0), \end{aligned} \tag{4}$$

where $\varphi_i(t), \phi_j(t) \subset \mathcal{X}$ denote the real-valued piecewise continuous functions on $[-\tau, 0]$.

To investigate the Mittag–Leffler synchronization between master neural network and slave neural network, we refer to system (2) as the master system, while the slave system takes the following form:

$$\begin{aligned} {}_0^C D_t^q \tilde{x}_i(t) = {} & -c_i^{(1)} \tilde{x}_i(t) + \sum_{j=1}^m a_{ji}^{(1)} f_j\big(\tilde{y}_j(t)\big) \\ & + \sum_{j=1}^m b_{ji}^{(1)} f_j\big(\tilde{y}_j(t - \eta_{ji}(t))\big) + I_i^{(1)} + u_i^{(1)}(t), \quad t \neq t_k, \end{aligned} \tag{5a}$$

$$\Delta \tilde{x}_i(t) = \gamma_k^{(1)}(\tilde{x}_i(t)), \quad t = t_k, \quad i = 1, 2, \dots, n, \ k = 1, 2, \dots,$$

$$
\begin{aligned}
{}_0^C D_t^q \tilde{y}_j(t) &= -c_j^{(2)} \tilde{y}_j(t) + \sum_{i=1}^{n} a_{ij}^{(2)} g_i\big(\tilde{x}_i(t)\big) \\
&\quad + \sum_{i=1}^{n} b_{ij}^{(2)} g_i\big(\tilde{x}_i(t-\sigma_{ij}(t))\big) + I_j^{(2)} + u_j^{(2)}(t), \quad t \neq t_k, \\
\Delta \tilde{y}_i(t) &= \gamma_k^{(2)}(\tilde{y}_i(t)), \quad t = t_k, \quad j = 1, 2, \ldots, m,\ k = 1, 2, \ldots,
\end{aligned}
\tag{5b}
$$

with the initial condition $\tilde{x}_i(t) = \tilde{\varphi}_i(t)$, $\tilde{y}_j(t) = \tilde{\phi}_j(t)$, $t \in [-\tau, 0]$.

Let $e_i(t) = \tilde{x}_i(t) - x_i(t)$, $\tilde{e}_j(t) = \tilde{y}_j(t) - y_j(t)$ $(i = 1, 2, \ldots, n; j = 1, 2, \ldots, m)$ be the synchronization errors. From master system (2) and slave system (5) the error system follows that

$$
\begin{aligned}
{}_0^C D_t^q e_i(t) &= -c_i^{(1)} e_i(t) + \sum_{j=1}^{m} a_{ji}^{(1)} f_j\big(\tilde{e}_j(t)\big) \\
&\quad + \sum_{j=1}^{m} b_{ji}^{(1)} f_j\big(\tilde{e}_j\big(t-\eta_{ji}(t)\big)\big) + u_i^{(1)}, \quad t \neq t_k, \\
\Delta e_i(t) &= \gamma_k^{(1)}(e_i(t)), \quad t = t_k, \quad i = 1, 2, \ldots, n,\ k = 1, 2, \ldots, \\
{}_0^C D_t^q \tilde{e}_j(t) &= -c_j^{(2)} \tilde{e}_j(t) + \sum_{i=1}^{n} a_{ij}^{(2)} g_i\big(e_i(t)\big) \\
&\quad + \sum_{i=1}^{n} b_{ij}^{(2)} g_i\big(e_i\big(t-\sigma_{ij}(t)\big)\big) + u_j^{(2)}, \quad t \neq t_k, \\
\Delta \tilde{e}_j(t) &= \gamma_k^{(2)}(\tilde{e}_j(t)), \quad t = t_k, \quad j = 1, 2, \ldots, m,\ k = 1, 2, \ldots,
\end{aligned}
\tag{6}
$$

where $f_j(\tilde{e}_j(t)) = f_j(\tilde{y}_j(t)) - f_j(y_j(t))$, $g_i(e_i(t)) = g_i(\tilde{x}_i(t)) - g_i(x_i(t))$.

Before the prove of Mittag–Leffler synchronization, we introduce the following definitions and lemmas.

Definition 1. (See [32].) System (2) has an equilibrium $(x_1^*, x_2^*, \ldots, x_n^*, y_1^*, y_2^*, \ldots, y_m^*)^{\mathrm{T}} \in \mathbb{R}^{n+m}$ if and only if

$$
\begin{aligned}
-c_i^{(1)} x_i^* + \sum_{j=1}^{m} a_{ji}^{(1)} f_j(y_j^*) + \sum_{j=1}^{m} b_{ji}^{(1)} f_j(y_j^*) + I_i^{(1)} = 0, \quad i = 1, 2, \ldots, n, \\
-c_j^{(2)} y_j^* + \sum_{i=1}^{n} a_{ij}^{(2)} g_i(x_i^*) + \sum_{i=1}^{n} b_{ij}^{(2)} g_i(x_i^*) + I_j^{(2)} = 0, \quad j = 1, 2, \ldots, m,
\end{aligned}
$$

and the impulsive jumps $\gamma_k^{(1)}(x_i(t_k))$ and $\gamma_k^{(2)}(y_j(t_k))$ satisfy

$$
\gamma_k^{(1)}(x_i^*) = 0, \quad \gamma_k^{(2)}\big(y_j^*\big) = 0, \quad i = 1, 2, \ldots, n,\ j = 1, 2, \ldots, m,\ k = 1, 2, \ldots .
$$

Definition 2. (See [20].) For any $t \geqslant t_0$, the Caputo fractional derivative of order q ($0 < q < 1$) with the lower limit t_0 for a function $f(t) \in C^1([t_0, b], \mathbb{R})$ ($b > t_0$) is defined as

$$ {}_{t_0}^{C}D_t^q f(t) = \frac{1}{\Gamma(1-q)} \int_{t_0}^{t} \frac{f'(\theta)}{(t-\theta)^q} \,\mathrm{d}\theta \quad (\Gamma \text{ denotes the gamma function.}) $$

Definition 3. (See [17].) Mittag–Leffler function is usually used in the solutions of fractional-order systems, which is defined as follows:

$$ E_q(z) = \sum_{k=0}^{\infty} \frac{z^k}{\Gamma(kq+1)}, \quad q > 0,\ z \in \mathbb{C}. $$

Lemma 1. (*See* [17].) *For the system* ${}_0^{C}D_t^q x(t) = f(t,x)$*, the solution is said to be Mittag–Leffler stable if*

$$ \big\|x(t)\big\| \leqslant \big\{ m\big[x(0)\big] E_q\big(-\lambda t^q\big) \big\}^b, $$

where fractional order $q \in (0,1)$*,* $\lambda \geqslant 0$*,* $b > 0$*,* $m(0) = 0$*,* $m(x) \geqslant 0$*, and* $m(x)$ *is locally Lipschitz on* $x \in \mathbb{R}^n$ *with Lipschitz constant* m_0*.*

Lemma 2. (*See* [7].) *Let* $V(t)$ *be a continuous function on* $[0, +\infty)$ *and satisfies*

$$ {}_0^{C}D_t^q V(t) \leqslant -\lambda V(t), \quad t > 0, $$

where $0 < q < 1$ *and* λ *is a constant. Then* $V(t) \leqslant V(0) E_q(-\lambda t^q)$*,* $t \in [0, +\infty)$*.*

2.2 Synchronization conditions via linear feedback controller

In this section, we investigate the Mittag–Leffler synchronization scheme for system (2). By designing linear feedback controllers, Mittag–Leffler synchronization between master system (2) and slave system (5) is established based on fractional calculus theory and Lyapunov functional method.

Design a linear feedback control strategy for slave system (5) by the following forms:

$$ \begin{aligned} u_i^{(1)}(t) &= -h_i^{(1)}(t) e_i(t), \quad i = 1, 2, \ldots, n, \\ u_j^{(2)}(t) &= -h_j^{(2)}(t) \tilde{e}_j(t), \quad j = 1, 2, \ldots, m, \end{aligned} \tag{7} $$

where $h_i^{(1)}(t), h_j^{(2)}(t) > 0$ are time-dependent control gains that will be determined later. Combining the linear feedback controllers (7) and condition (H2), error system (6) follows that

$$ \begin{aligned} {}_0^{C}D_t^q e_i(t) = {} & -c_i^{(1)} e_i(t) + \sum_{j=1}^{m} a_{ji}^{(1)} f_j\big(\tilde{e}_j(t)\big) \\ & + \sum_{j=1}^{m} b_{ji}^{(1)} f_j\big(\tilde{e}_j\big(t - \eta_{ji}(t)\big)\big) - h_i^{(1)}(t) e_i(t), \quad t \neq t_k, \end{aligned} \tag{8a} $$

$$ \Delta e_i(t) = -\lambda_{ik}^{(1)} e_i(t_k), \quad t = t_k, \quad i = 1, 2, \ldots, n,\ k = 1, 2, \ldots, $$

$$
\begin{aligned}
{}_0^C D_t^q \tilde{e}_j(t) &= -c_j^{(2)} \tilde{e}_j(t) + \sum_{i=1}^{n} a_{ij}^{(2)} g_i\big(e_i(t)\big) \\
&\quad + \sum_{i=1}^{n} b_{ij}^{(2)} g_i\big(e_i\big(t-\sigma_{ij}(t)\big)\big) - h_j^{(2)}(t)\tilde{e}_j(t), \quad t \neq t_k, \\
\Delta\tilde{e}_j(t) &= -\lambda_{jk}^{(2)} \tilde{e}_j(t_k), \quad t = t_k, \quad j = 1,2,\ldots,m,\ k = 1,2,\ldots .
\end{aligned} \tag{8b}
$$

According to Definition 1, $(e_i^*, \tilde{e}_j^*)^{\mathrm{T}} = (0,0,\ldots,0)^{\mathrm{T}} \in \mathbb{R}^{n+m}$ is an equilibrium of error system (8). Besides, the impulsive operators satisfy $\gamma_k^{(1)}(e_i^*) = 0$, $\gamma_k^{(2)}(\tilde{e}_j^*) = 0$, $i = 1,2,\ldots,n$, $j = 1,2,\ldots,m$, $k = 1,2,\ldots$. Suppose that the initial value $(e_i(0), \tilde{e}_j(0))^{\mathrm{T}}$ satisfies that $e_i(0) \neq 0$ and $\tilde{e}_j(0) \neq 0$.

Theorem 1. *Suppose that conditions* (H1)–(H4) *hold, then master system* (2) *can achieve Mittag–Leffler synchronization with slave system* (5) *under the linear feedback controllers* (7) *if there exist two positive constants* ρ_1, ρ_2 *such that* $\rho_2 > \rho_1 > 0$, *where*

$$
\begin{aligned}
\rho_1 &= \max\left\{ \max_{1\leqslant i\leqslant n}\left[L_i^g \sum_{j=1}^{m} \big|b_{ij}^{(2)}\big| \right], \max_{1\leqslant j\leqslant m}\left[L_j^f \sum_{i=1}^{n} \big|b_{ji}^{(1)}\big| \right] \right\}, \\
\rho_2 &= \min\left\{ \min_{1\leqslant i\leqslant n}\left[c_i^{(1)} + h_i^{(1)}(t) - L_i^g \sum_{j=1}^{m} \big|a_{ij}^{(2)}\big| \right], \right. \\
&\qquad \left. \min_{1\leqslant j\leqslant m}\left[c_j^{(2)} + h_j^{(2)}(t) - L_j^f \sum_{i=1}^{n} \big|a_{ji}^{(1)}\big| \right] \right\}.
\end{aligned} \tag{9}
$$

Proof. Define a piecewise continuous Lyapunov functional as follows:

$$
V\big(t, e(t), \tilde{e}(t)\big) = \sum_{i=1}^{n} \big|e_i(t)\big| + \sum_{j=1}^{m} \big|\tilde{e}_j(t)\big|. \tag{10}
$$

Case 1. For $t = t_k$, from (3) and (H2) we have

$$
\begin{aligned}
V\big(t_k^+, e\big(t_k^+\big), \tilde{e}\big(t_k^+\big)\big) &= \sum_{i=1}^{n} \big|e_i(t_k) + \gamma_k^{(1)}\big(e_i\big(t_k\big)\big)\big| + \sum_{j=1}^{m} \big|\tilde{e}_j(t_k) + \gamma_k^{(2)}\big(\tilde{e}_j(t_k)\big)\big| \\
&= \sum_{i=1}^{n} \big|e_i(t_k) - \lambda_{ik}^{(1)} e_i(t_k)\big| + \sum_{j=1}^{m} \big|\tilde{e}_j\big(t_k\big) - \lambda_{jk}^{(2)} \tilde{e}_j(t_k)\big|.
\end{aligned}
$$

Noting that $\lambda_{ik}^{(1)}, \lambda_{jk}^{(2)} \in (0,2)$, we obtain that

$$
\begin{aligned}
V\big(t_k^+, e\big(t_k^+\big), \tilde{e}\big(t_k^+\big)\big) &\leqslant \sum_{i=1}^{n} \big|1 - \lambda_{ik}^{(1)}\big|\big|e_i(t_k)\big| + \sum_{j=1}^{m} \big|1 - \lambda_{jk}^{(2)}\big|\big|\tilde{e}_j(t_k)\big| \\
&\leqslant \sum_{i=1}^{n} \big|e_i(t_k)\big| + \sum_{j=1}^{m} \big|\tilde{e}_j(t_k)\big| \\
&= V\big(t_k, e(t_k), \tilde{e}(t_k)\big), \quad k = 1,2,\ldots .
\end{aligned}
$$

Case 2. For $t \neq t_k$, namely, $t \in [t_{k-1}, t_k)$, the Caputo fractional derivative of (10) is

$$ {}_0^C D_t^\alpha V\big(t, e(t), \tilde{e}(t)\big) = {}_0^C D_t^\alpha \left[\sum_{i=1}^{n} \big|e_i(t)\big| \right] + {}_0^C D_t^\alpha \left[\sum_{j=1}^{m} \big|\tilde{e}_j(t)\big| \right]. \tag{11} $$

Next, the fractional-order derivatives along the solutions of first and third equations of system (8) are calculated as follows:

$$ \begin{aligned} {}_0^C D_t^q \big|e_i(t)\big| &\leqslant -c_i^{(1)} \big|e_i(t)\big| + \sum_{j=1}^{m} \big|a_{ji}^{(1)}\big| \big|f_j\big(\tilde{e}_j(t)\big)\big| \\ &\quad + \sum_{j=1}^{m} \big|b_{ji}^{(1)}\big| \big|f_j\big(\tilde{e}_j\big(t-\eta_{ji}(t)\big)\big)\big| - h_i^{(1)}(t)\big|e_i(t)\big|, \\ {}_0^C D_t^q \big|\tilde{e}_j(t)\big| &\leqslant -c_j^{(2)} \big|\tilde{e}_j(t)\big| + \sum_{i=1}^{n} \big|a_{ij}^{(2)}\big| \big|g_i\big(e_i(t)\big)\big| \\ &\quad + \sum_{i=1}^{n} \big|b_{ij}^{(2)}\big| \big|g_i\big(e_i\big(t-\sigma_{ij}(t)\big)\big)\big| - h_j^{(2)}(t)\big|\tilde{e}_j(t)\big|. \end{aligned} \tag{12} $$

Following from (H1), (12) is changed into

$$ \begin{aligned} {}_0^C D_t^q \big|e_i(t)\big| &\leqslant -c_i^{(1)} \big|e_i(t)\big| + \sum_{j=1}^{m} \big|a_{ji}^{(1)}\big| L_j^f \big|\tilde{e}_j(t)\big| \\ &\quad + \sum_{j=1}^{m} \big|b_{ji}^{(1)}\big| L_j^f \big|\tilde{e}_j\big(t-\eta_{ji}(t)\big)\big| - h_i^{(1)}(t)\big|e_i(t)\big|, \\ {}_0^C D_t^q \big|\tilde{e}_j(t)\big| &\leqslant -c_j^{(2)} \big|\tilde{e}_j(t)\big| + \sum_{i=1}^{n} \big|a_{ij}^{(2)}\big| L_i^g \big|e_i(t)\big| \\ &\quad + \sum_{i=1}^{n} \big|b_{ij}^{(2)}\big| L_i^g \big|e_i\big(t-\sigma_{ij}(t)\big)\big| - h_j^{(2)}(t)\big|\tilde{e}_j(t)\big|. \end{aligned} \tag{13} $$

Substituting (13) into (11) yields

$$ \begin{aligned} {}_0^C D_t^\alpha V\big(t, e(t), \tilde{e}(t)\big) &\leqslant -\min_{1\leqslant i\leqslant n} \left[c_i^{(1)} + h_i^{(1)}(t) - L_i^g \sum_{j=1}^{m} \big|a_{ij}^{(2)}\big| \right] \sum_{i=1}^{n} \big|e_i(t)\big| \\ &\quad - \min_{1\leqslant j\leqslant m} \left[c_j^{(2)} + h_j^{(2)}(t) - L_j^f \sum_{i=1}^{n} \big|a_{ji}^{(1)}\big| \right] \sum_{j=1}^{m} \big|\tilde{e}_j(t)\big| \\ &\quad + \max_{1\leqslant i\leqslant n} \left[L_i^g \sum_{j=1}^{m} \big|b_{ij}^{(2)}\big| \right] \sum_{i=1}^{n} \sup_{t-\tau\leqslant s\leqslant t} \big|e_i(s)\big| \\ &\quad + \max_{1\leqslant j\leqslant m} \left[L_j^f \sum_{i=1}^{n} \big|b_{ji}^{(1)}\big| \right] \sum_{j=1}^{m} \sup_{t-\tau\leqslant s\leqslant t} \big|\tilde{e}_j(s)\big|. \end{aligned} \tag{14} $$

From (9) in Theorem 1 we have

$$ {}_0^C D_t^\alpha V\big(t, e(t), \tilde{e}(t)\big) \leqslant -\rho_2 V\big(t, e(t), \tilde{e}(t)\big) + \rho_1 \sup_{t-\tau \leqslant s \leqslant t} V\big(s, e(s), \tilde{e}(s)\big). \tag{15} $$

For any solution $(\mathrm{e}^{\mathrm{T}}(t), \tilde{e}^{\mathrm{T}}(t))^{\mathrm{T}}$ of error system (8), which satisfies the following Razumikhin condition [31]

$$ V\big(s, e(s), \tilde{e}(s)\big) \leqslant V\big(t, e(t), \tilde{e}(t)\big), \quad t - \tau \leqslant s \leqslant t, $$

there exists a real positive number λ satisfying $\lambda \leqslant \rho_2 - \rho_1$ such that

$$ {}_0^C D_t^\alpha \big\{V\big(t, e(t), \tilde{e}(t)\big)\big\} \leqslant -\lambda V\big(t, e(t), \tilde{e}(t)\big), \quad t > 0,\ t \neq t_k. $$

According to Lemma 2, we obtain that

$$ V\big(t, e(t), \tilde{e}(t)\big) \leqslant V\big(0, e(0), \tilde{e}(0)\big) E_q\big(-\lambda t^q\big) \quad \forall t \in [0, +\infty). \tag{16} $$

From Lemma 1 we conclude that master system (2) achieve Mittag–Leffler synchronization with slave system (5) under the linear feedback controllers (7). In the next section, we focus on finding time-dependent control gains by optimal control methods. □

Remark 1. When the Caputo fractional derivative order q equals to 1, fractional-order error system (8) become a integer-order system. The condition of Mittag–Leffler synchronization (16) is transformed into

$$ V\big(t, e(t), \tilde{e}(t)\big) \leqslant V\big(0, e(0), \tilde{e}(0)\big) \mathrm{e}^{-\lambda t} \quad \forall t \in [0, +\infty), $$

which implies that the corresponding integer-order system realizes the exponential synchronization.

3 Optimal linear feedback controller

In this section, we aim to minimize the accumulative errors within the limitation of actuator saturation based on Pontryagin's maximum principle with delay [3, 16].

3.1 Statement of optimal control problem

Without loss of generality, we focus on a four-neuron impulsive fractional-order BAM neural network, where $\eta_{ji}(t), \sigma_{ij}(t)$ are set as the constant τ and $m = n = 2$ in error system (8). Next, we discuss the existence of the optimal control solutions. Let $x(t) = (e_1(t), e_2(t), \tilde{e}_1(t), \tilde{e}_2(t))$ be the state variable. Define a control function set as

$$ u(t) = \big(h_1^{(1)}(t), h_2^{(1)}(t), h_1^{(2)}(t), h_2^{(2)}(t)\big). $$

Due to the limitations of synchronization conditions and actuator saturation, each of control outputs has upper bound. The saturation function is defined as

$$\operatorname{sat}\big(u(t)\big) = \big[\operatorname{sat}\big(u_1^{(1)}(t)\big), \operatorname{sat}\big(u_2^{(1)}(t)\big), \operatorname{sat}\big(u_1^{(2)}(t)\big), \operatorname{sat}\big(u_2^{(2)}(t)\big)\big]^{\mathrm{T}} \tag{17}$$

in which

$$\operatorname{sat}\big(u_i^{(j)}(t)\big) = \operatorname{sign}\big(u_i^{(j)}(t)\big) \min\big\{\big|u_i^{(j)}(t)\big|, \bar{u}_i^{(j)}\big\}, \quad i = 1, 2,\ j = 1, 2,$$

where $\bar{u}_1^{(1)}, \bar{u}_2^{(1)}, \bar{u}_1^{(2)}, \bar{u}_2^{(2)}$ are the saturation levels for the corresponding actuators, respectively. To better state the optimal control problem, we firstly introduce two sets, namely, the sets of admissible trajectories and control. The set $\mathcal{X}$ of admissible trajectories is given by

$$\mathcal{X} = \big\{x(\cdot) \in W^{1,1}\big([0,T], \mathbb{R}^4\big) \;\big|\; \text{(4) and (8) are satisfied}\big\},$$

and the admissible control set $\mathcal{U}$ is given by

$$\mathcal{U} = \big\{u(\cdot) \in L^{\infty}\big([0,T], \mathbb{R}^4\big) \;\big|\; \text{(17) is satisfied for all } t \in [0,T]\big\}.$$

From [25] we consider the following objective functional:

$$J\big(x(\cdot), u(\cdot)\big) = \int_0^T f\big(t, u(t), x(t)\big)\,\mathrm{d}t, \tag{18}$$

where

$$\begin{aligned} f\big(t, u(t), x(t)\big) = {} & A_1 \sum_{i=1}^{n} \big|e_i(t)\big| + A_2 \sum_{j=1}^{m} \big|\tilde{e}_j(t)\big| \\ & + B_1 \sum_{i=1}^{n} \big(e_i(t) h_i^{(1)}(t)\big)^2 + B_2 \sum_{j=1}^{m} \big(\tilde{e}_j(t) h_j^{(2)}(t)\big)^2. \end{aligned}$$

Thereinto, A_1 and A_2 denote the weight constants for the accumulative errors, while B_1 and B_2 are the weight constants for the outputs of linear feedback controllers. Accumulative error means that as time goes on, the errors between the master system and the slave system accumulate gradually.

The optimal control problem consists of determining the vector function $x^{\diamond}(\cdot) = (\mathrm{e}_1^{\diamond}(t), \mathrm{e}_2^{\diamond}(t), \tilde{e}_1^{\diamond}(t), \tilde{e}_2^{\diamond}(t)) \in \mathcal{X}$ associated with an admissible control $u^{\diamond}(\cdot) \in \mathcal{U}$ on the time interval $[0,T]$, minimizing the objective functional J, namely,

$$J\big(x^{\diamond}(\cdot), u^{\diamond}(\cdot)\big) = \min_{x(\cdot), u(\cdot) \in \mathcal{X} \times \mathcal{U}} J\big(x(\cdot), u(\cdot)\big). \tag{19}$$

3.2 Characterization of optimal control

In this subsection, by constructing the Hamiltonian H and then applying the Pontryagin's maximum principle, we derive the first-order necessary conditions for the existence of

optimal control. The Hamiltonian is given by

$$H\big(t,u(t),x(t),\lambda(t)\big)=f\big(t,u(t),x(t)\big)+\lambda\,{}_0^C D_t^q x(t).$$

For more details about how to construct the Hamiltonian, please see [1, 11].

Let $u^\diamond(\cdot)=(h_1^{(1)}(t),h_2^{(1)}(t),h_1^{(2)}(t),h_2^{(2)}(t))$ be the optimal control and $x^\diamond(\cdot)=(\mathrm{e}_1^\diamond(t),\mathrm{e}_2^\diamond(t),\tilde{e}_1^\diamond(t),\tilde{e}_2^\diamond(t))$ be the corresponding optimal trajectory. According to the Pontryagin maximum principle [21], if $u^\diamond(\cdot)\in\mathcal{U}$ is optimal for problem (19) with fixed final time T, there exists a nontrivial absolutely continuous mapping $\lambda:[0,T]\to\mathbb{R}^4$, $\lambda(t)=(\lambda_1(t),\lambda_2(t),\lambda_3(t),\lambda_4(t))$ called the adjoint vector. From [5,21] it is not difficult to show the following theorem.

Theorem 2. *The optimal control problem* (19) *with fixed final time T admits a unique optimal solution $(\mathrm{e}_1^\diamond(t),\mathrm{e}_2^\diamond(t),\tilde{e}_1^\diamond(t),\tilde{e}_2^\diamond(t))$ associated with an optimal control $u^\diamond(t)$ for $t\in[0,T]$. Moreover, there exist adjoint functions $\lambda_i^\diamond(\cdot)$ $(i=1,\dots,4)$ such that*

$$\begin{aligned}
\frac{\partial\lambda_1(t)}{\partial t}&=-\left(\frac{\partial H}{\partial e_1(t)}+\chi_{[0,\,T-\tau]}\frac{\partial H}{\partial e_1(t-\tau)}\bigg|_{t=t+\tau}\right),\\
\frac{\partial\lambda_2(t)}{\partial t}&=-\left(\frac{\partial H}{\partial e_2(t)}+\chi_{[0,\,T-\tau]}\frac{\partial H}{\partial e_2(t-\tau)}\bigg|_{t=t+\tau}\right),\\
\frac{\partial\lambda_3(t)}{\partial t}&=-\left(\frac{\partial H}{\partial \tilde{e}_1(t)}+\chi_{[0,\,T-\tau]}\frac{\partial H}{\partial \tilde{e}_1(t-\tau)}\bigg|_{t=t+\tau}\right),\\
\frac{\partial\lambda_4(t)}{\partial t}&=-\left(\frac{\partial H}{\partial \tilde{e}_2(t)}+\chi_{[0,\,T-\tau]}\frac{\partial H}{\partial \tilde{e}_2(t-\tau)}\bigg|_{t=t+\tau}\right)
\end{aligned}\tag{20}$$

with transversality conditions $\lambda_i^\diamond(T)=0$, $i=1,\dots,4$, where $\chi_{[a,b]}(t)$ is the characteristic function defined by

$$\chi_{[a,b]}=\begin{cases}1 & \text{if } t\in[a,b],\\ 0 & \text{otherwise}.\end{cases}$$

From the optimality conditions it follows that

$$\frac{\partial H}{\partial u}\big(t,x(t),u(t),\lambda(t)\big)=0,$$

where

$$\begin{aligned}
\bar{h}_1^{(1)}(t)&=\frac{\lambda_1(t)}{2B_1e_1(t)}, & \bar{h}_2^{(1)}(t)&=\frac{\lambda_2(t)}{2B_1e_2(t)},\\
\bar{h}_1^{(2)}(t)&=\frac{\lambda_3(t)}{2B_2\tilde{e}_1(t)}, & \bar{h}_2^{(2)}(t)&=\frac{\lambda_4(t)}{2B_2\tilde{e}_2(t)}.
\end{aligned}$$

Proof. To obtain the optimal control solutions $u^\diamond(t)$, the objective function (18) is rewritten as

$$J(u)=\int_0^T\big[H\big(t,u(t),x(t),\lambda(t)\big)-\lambda(t)\big({}_0^C D_t^q x(t)\big)\big]\,\mathrm{d}t,\tag{21}$$

where λ is the Lagrange multiplier vector known as the co-state variable. The variation of (21) yields

$$\delta J = \int_0^T \left[\delta x \frac{\partial H}{\partial x} + \delta u \frac{\partial H}{\partial u} + \delta\lambda \frac{\partial H}{\partial \lambda} - (\delta\lambda){}_0^C D_t^q x - \lambda\delta\big({}_0^C D_t^q x\big)\right] \mathrm{d}t, \tag{22}$$

where δx, δu and $\delta\lambda$ are the variations of x, u and λ, respectively. Using the integration by parts formula for Caputo fractional derivative [11], we have

$$\int_0^T \lambda(t)\delta\big({}_0^C D_t^q x\big)\mathrm{d}t = \big({}_t I_T^{1-q}\lambda(t)\big)\delta x(t)\big|_0^T - \int_0^T \delta x\big({}_t D_T^q \lambda(t)\big)\mathrm{d}t, \tag{23}$$

where ${}_0 D_t^q$ denotes the Riemann–Liouville derivative. Since $x(0)$ is specified in the optimal control, $\delta x(0) = 0$. Thus,

$$\begin{aligned}\delta J = \int_0^T \left[\delta x\left(\frac{\partial H}{\partial x} - {}_t D_T^q \lambda(t)\right) + \delta u \frac{\partial H}{\partial u} + \delta\lambda\left(\frac{\partial H}{\partial \lambda} - {}_0^C D_t^q x\right)\right] \mathrm{d}t \\ - \big({}_t I_T^{1-q}\lambda(t)\big)\delta x(t)\big|_{t=T}.\end{aligned} \tag{24}$$

The necessary condition for the fractional optimal control problem is $\delta J = 0$. This requires that the coefficients of x, u and λ in (24) be 0 simultaneously, namely,

$$\begin{aligned}&{}_0^C D_t^q x(t) = \frac{\partial H}{\partial \lambda}\big(t, x(t), u(t), \lambda(t)\big),\\ &{}_t D_T^q \lambda(t) = \frac{\partial H}{\partial x}\big(t, x(t), u(t), \lambda(t)\big),\\ &\frac{\partial H}{\partial u}\big(t, x(t), u(t), \lambda(t)\big) = 0,\\ &{}_t I_T^{1-q}\lambda(t)\big|_{t=T} = 0.\end{aligned} \tag{25}$$

Since λ is continuous, the condition ${}_t I_T^{1-\alpha}\lambda(t)|_{t=T} = 0$ implies $\lambda(T) = 0$. Therefore, according to the relation between Riemann–Liouville and Caputo derivatives, we obtain that

$${}_t D_T^q \left[\lambda(t) - \sum_{k=0}^{n-1} \frac{(t-T)^k}{k!}\lambda^{(k)}(T)\right] = {}_t^C D_T^q \lambda(t).$$

The necessary condition in (25) is equivalent to

$$\begin{aligned}&{}_0^C D_t^\alpha x(t) = \frac{\partial H}{\partial \lambda}\big(t, x(t), u(t), \lambda(t)\big),\\ &{}_t^C D_T^\alpha \lambda(t) = \frac{\partial H}{\partial x}\big(t, x(t), u(t), \lambda(t)\big),\\ &\frac{\partial H}{\partial u}\big(t, x(t), u(t), \lambda(t)\big) = 0,\\ &\lambda(T) = 0.\end{aligned} \tag{26}$$

□

Remark 2. The analysis of the optimal control problem in this section helps us set proper control gains according to different control purposes. Weight constants A_1, A_2, B_1 and B_2 in objective functional (18) are selected based on the control purposes, that is to say, if minimizing the accumulative errors are more important than restricting the outputs of controllers during the Mittag–Leffler synchronization, A_1 and A_2 should be set as larger values.

Remark 3. In [34], the control gains of linear feedback controllers are set as constants, which also ensures the global synchronization of the master-slave systems. But, in practical control progress, it is difficult to deliver arbitrarily large signals through real controllers. Besides, the control gains selected in [34] maybe not optimal, which cannot minimize the accumulative errors during the Mittag–Leffler synchronization. This problem also exists in the delayed-feedback controllers of [32] and the state feedback controllers of [35].

Remark 4. The time-dependent control gains in this subsection firstly satisfy the Mittag–Leffler synchronization conditions in Section 2.2, that is to say, the lower bounds of control gains are determined by the synchronization conditions.

4 Numerical simulations

In this section, we carry out some numerical simulations to illustrate the analytical predictions obtained in Sections 2 and 3. Based on the modified predictor-corrector algorithm [4, 8] and the forward-backward sweep method [14], we derive the time-dependent control gains, which minimizes the accumulative errors within the limitation of actuator saturation.

4.1 Numerical solutions of control gains

Consider a four-neuron impulsive fractional-order BAM neural network with synaptic transmission delay, where $m = n = 2$ in error system (8). Parameter values are set as follows:

$$\begin{bmatrix} c_1^{(1)} & 0 \\ 0 & c_2^{(1)} \end{bmatrix} = \begin{bmatrix} 0.4 & 0 \\ 0 & 0.6 \end{bmatrix}, \qquad \begin{bmatrix} c_1^{(2)} & 0 \\ 0 & c_2^{(2)} \end{bmatrix} = \begin{bmatrix} 0.5 & 0 \\ 0 & 0.8 \end{bmatrix},$$

$$\begin{bmatrix} a_{11}^{(1)} & a_{12}^{(1)} \\ a_{21}^{(1)} & a_{22}^{(1)} \end{bmatrix} = \begin{bmatrix} 1.5 & -0.6 \\ 0.8 & -0.5 \end{bmatrix}, \qquad \begin{bmatrix} a_{11}^{(2)} & a_{12}^{(2)} \\ a_{21}^{(2)} & a_{22}^{(2)} \end{bmatrix} = \begin{bmatrix} -1.5 & 0.5 \\ 2.5 & -0.8 \end{bmatrix},$$

$$\begin{bmatrix} b_{11}^{(1)} & b_{12}^{(1)} \\ b_{21}^{(1)} & b_{22}^{(1)} \end{bmatrix} = \begin{bmatrix} 1.2 & -0.4 \\ 0.7 & -0.8 \end{bmatrix}, \qquad \begin{bmatrix} b_{11}^{(2)} & b_{12}^{(2)} \\ b_{21}^{(2)} & b_{22}^{(2)} \end{bmatrix} = \begin{bmatrix} -1.8 & 0.4 \\ 2.2 & -0.7 \end{bmatrix},$$

$$\begin{bmatrix} \eta_{11}(t) & \eta_{11}(t) \\ \eta_{11}(t) & \eta_{11}(t) \end{bmatrix} = \begin{bmatrix} 0.5(1+\sin t) & 0.5(1+\cos t) \\ 0.5(1+\cos t) & 0.5(1+\sin t) \end{bmatrix},$$

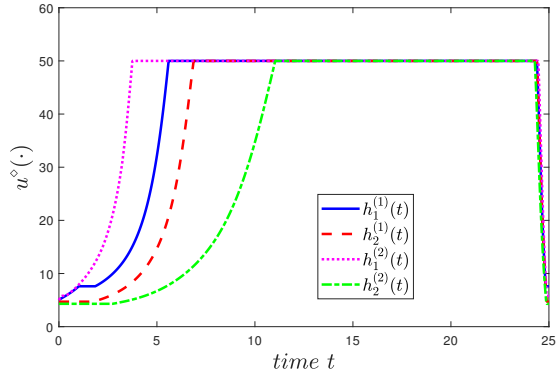

Figure 1. State trajectories of control gains $h_1^{(1)}(t)$, $h_2^{(1)}(t)$, $h_1^{(2)}(t)$, $h_2^{(2)}(t)$, respectively.

$$\begin{bmatrix} \sigma_{11}(t) & \sigma_{11}(t) \\ \sigma_{11}(t) & \sigma_{11}(t) \end{bmatrix} = \begin{bmatrix} 0.5(1+\cos t) & 0.5(1+\sin t) \\ 0.5(1+\sin t) & 0.5(1+\cos t) \end{bmatrix}.$$

Besides, $f_j(\cdot)$ and $g_i(\cdot)$ are set as $\tanh(\cdot)$. The initial conditions for master system (2) and slave system (5) are $(-0.4, 0.1, -0.3, 0.2)$ and $(-0.3, 0.2, -0.2, 0.3)$, respectively. From the synchronization conditions in Section 2.2 we obtain that the lower bounds of control gains: $\check{h}_1^{(1)} = 7.6$, $\check{h}_2^{(1)} = 4.7$, $\check{h}_1^{(2)} = 5.8$, $\check{h}_2^{(2)} = 4.3$. Considering the actuator saturation, each of control outputs has limitation, thus we set $\bar{u}_1^{(1)} = \bar{u}_2^{(1)} = \bar{u}_1^{(2)} = \bar{u}_2^{(2)} = 0.5$ [15]. Besides, we assume that the upper bound of control gain is 50. The order of fractional derivative is set as 0.8.

In the initial stage of Mittag–Leffler synchronization, the errors are relatively large in system (8). Due to the actuator saturation, as shown in Fig. 1, control gains are correspondingly small. Gradually, as the errors decrease, control gains increase to upper bounds for minimizing the accumulative errors. At last, the dynamical behaviors of system (8) approach to asymptotical stability. Control outputs are less necessary and could be reduced to the lower bounds.

4.2 Dynamics behaviors of Mittag–Leffler synchronization

In this section, we mainly focus on the dynamical behaviors of master system (2) and slave system (5). As the initial value $(e_i(0), \tilde{e}_j(0))^{\mathrm{T}}$ satisfies that $e_i(0) \neq 0$ and $\tilde{e}_j(0) \neq 0$, fractional master system (2) cannot achieve Mittag–Leffler synchronization with fractional slave system (5) without control. Once introducing the optimal linear feedback controllers to slave system (5), in Fig. 2, slave system (5) well synchronizes with master system (2). It is not difficult to find the state trajectories of master system (2) or slave system (5) change suddenly at some points, which is induced by the impulsive effect.

Ye et al. [32] proposed the delayed-feedback controllers to realize the global Mittag–Leffler synchronization for fractional-order BAM neural networks. In this subsection,

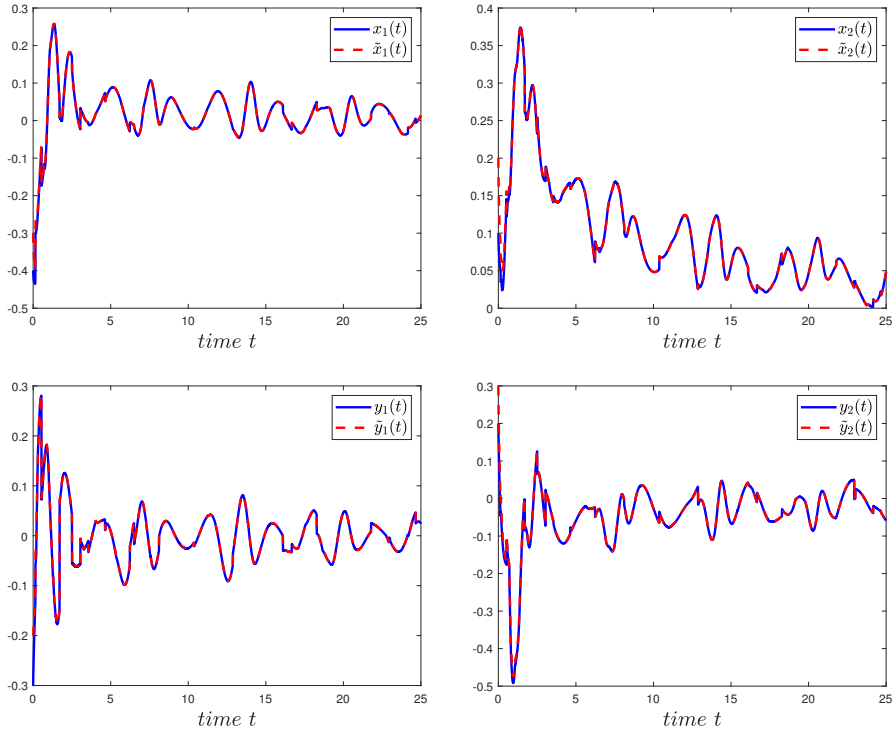

Figure 2. State trajectories of master system (2) and slave system (5) under optimal linear feedback control with $q = 0.8$.

we compare the optimal linear control with the delayed-feedback control. Firstly, we construct the following delayed-feedback controllers inspired by Ye et al. [32]:

$$
\begin{aligned}
u_1^{(1)}(t) &= -5e_1(t) - 15\operatorname{sgn}\big(e_1(t)\big)\big|e_1(t-1)\big|,\\
u_2^{(1)}(t) &= -10e_2(t) - 15\operatorname{sgn}\big(e_2(t)\big)\big|e_2(t-1)\big|,\\
u_1^{(2)}(t) &= -20\bar{e}_1(t) - 15\operatorname{sgn}\big(\bar{e}_1(t)\big)\big|\tilde{e}_1(t-1)\big|,\\
u_2^{(2)}(t) &= -15\bar{e}_2(t) - 15\operatorname{sgn}\big(\bar{e}_2(t)\big)\big|\tilde{e}_2(t-1)\big|.
\end{aligned}
$$

Figure 3 describes the dynamical behaviors of error system (6) under the optimal linear feedback control and the delayed-feedback control, respectively. As we can see, the transition process of error states with the optimal linear feedback control is smooth and steady relatively, while under the delayed-feedback control, the error states oscillate in the transition process. The only disadvantage of the optimal linear feedback control is that the transition time is a little bit longer.

Remark 5. As for the forward-backward sweep method, the values for λ are not needed to solve the differential equation for x. Then the algorithm terminates when there is

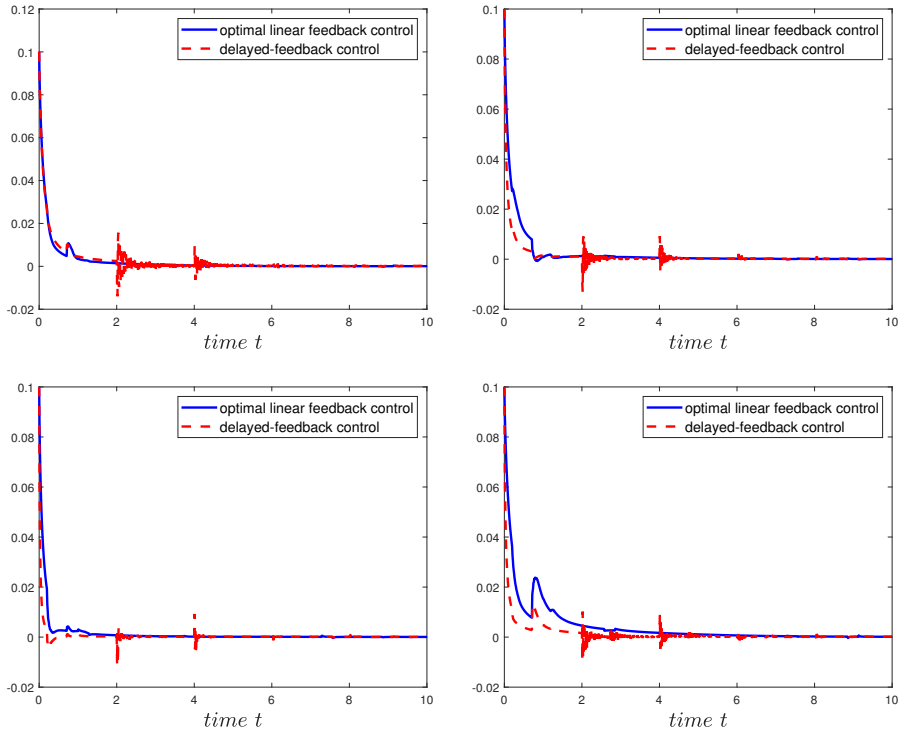

Figure 3. State trajectories of error system (6) under optimal linear feedback control and delayed-feedback control, respectively.

sufficient agreement between the states, co-states, and controls of two passes through the approximation loop, which is easy to program and converges faster [14]. Daftardar-Gejji et al. [4, 8] modified the fractional Adams method by applying the iterative method that is called the modified predictor-corrector algorithm. The predictor terms are used to approximate the corresponding terms in the corrector formula, and the method is relatively accurate and time-efficient.

Remark 6. In Fig. 4, we carry out a comparison between the fractional error system (6) and the corresponding integer-order system. It is not difficult to find that the transition process of error states with $q = 0.8$ is smoother and steadier than that with $q = 1$.

5 Conclusion

In this paper, we have investigated the Mittag–Leffler synchronization for impulsive fractional-order BAM neural networks with optimal linear feedback controllers. By constructing Lyapunov functional, sufficient conditions are established to ensure the Mittag–Leffler synchronization. Based on Pontryagin's maximum principle with delay, time-dependent

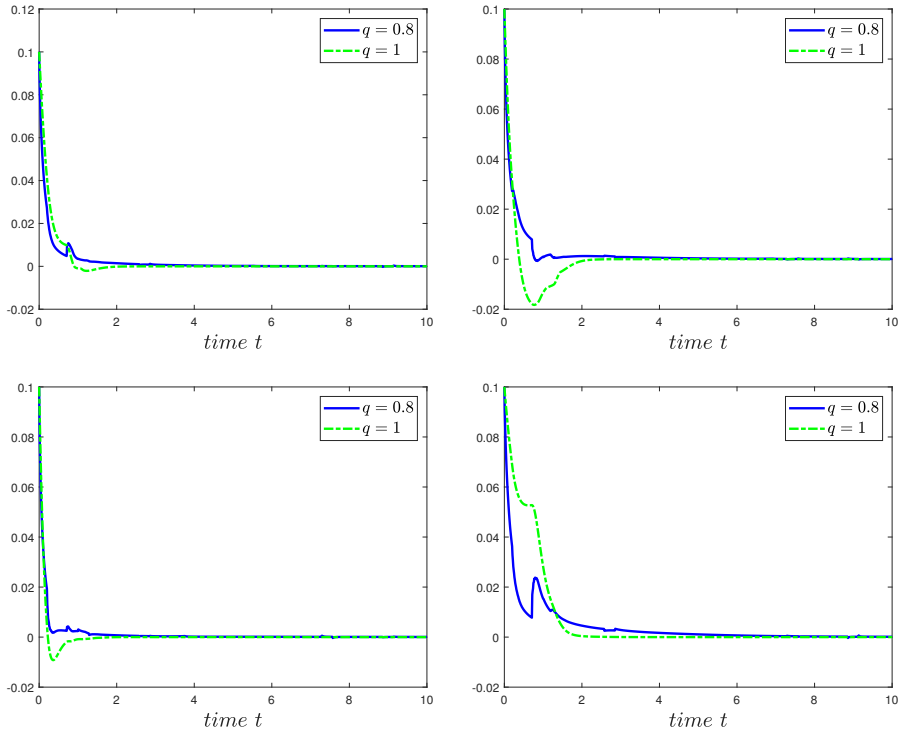

Figure 4. State trajectories of error system (6) with $q = 1$ and $q = 0.8$, respectively.

control gains are obtained, which minimizes the accumulative errors within the limitation of actuator saturation. As shown in numerical simulations, under optimal linear feedback controllers, slave system (5) well synchronizes with master system (2).

The objective functional in Section 3.1 consists of the accumulative errors and the controller outputs, and the obtained optimal control gains can minimize the accumulative errors during the Mittag–Leffler synchronization. To achieve different control effects, we can choose some other parameters that characterize the process of Mittag–Leffler synchronization, such as rise time t_r and maximum overshoot σ_p. Rise time t_r is the time from the beginning to the time when the state of the error system first reaches the steady-state value, while maximum overshoot σ_p measures whether the synchronization process is smooth. However, it is complicated to solve t_r and σ_p in error system (6) and we leave it for further investigation.

Acknowledgment. We would like to thank the referees and the editor for their careful reading of the original manuscript and their valuable comments and suggestions that improved the presentation of this work.

References

1. O.P. Agrawal, A general formulation and solution scheme for fractional optimal control problems, *Nonlinear Dyn.*, **38**(1):323–337, 2004, https://doi.org/10.1007/s11071-004-3764-6.
2. T.J. Anastasio, The fractional-order dynamics of brainstem vestibule-oculomotor neurons, *Biol. Cybern.*, **72**:69–79, 1994, https://doi.org/10.1007/BF00206239.
3. E. Bashier, K. Patidar, Optimal control of an epidemiological model with multiple time delays, *Appl. Math. Comput.*, **292**:47–56, 2017, https://doi.org/10.1016/j.amc.2016.07.009.
4. S. Bhalekar, D. Varsha, A predictor-corrector scheme for solving nonlinear delay differential equations of fractional order, *J. Fract. Calc. Appl.*, **5**:1–9, 2011.
5. L. Cesari, *Optimization—Theory and Applications*, Springer, New York, 1983.
6. J. Chen, C. Li, X. Yang, Global Mittag–Leffler projective synchronization of nonidentical fractional-order neural networks with delay via sliding mode control, *Neurocomputing*, **313**:324–332, 2018, https://doi.org/10.1016/j.neucom.2018.06.029.
7. J. Chen, Z. Zeng, P. Jiang, Global Mittag–Leffler stability and synchronization of memristor-based fractional-order neural networks, *Neural Netw.*, **51**:1–8, 2014, https://doi.org/10.1016/j.neunet.2013.11.016.
8. V. Daftardar-Gejji, Y. Sukale, S. Bhalekar, Solving fractional delay differential equations: A new approach, *Fract. Calc. Appl. Anal.*, **18**:400–418, 2015, https://doi.org/10.1515/fca-2015-0026.
9. X. Ding, J. Cao, X. Zhao, F.E. Alsaadi, Mittag–Leffler synchronization of delayed fractional-order bidirectional associative memory neural networks with discontinuous activations: State feedback control and impulsive control schemes, *Proc. R. Soc. Lond., Ser. A, Math. Phys. Eng. Sci.*, **473**:20170322, 2017, https://doi.org/10.1098/rspa.2017.0322.
10. T. Hu, Z. He, X. Zhang, S. Zhong, Global synchronization of time-invariant uncertainty fractional-order neural networks with time delay, *Neurocomputing*, **339**:45–58, 2019, https://doi.org/10.1016/j.neucom.2019.02.020.
11. H. Kheiri, M. Jafari, Optimal control of a fractional-order model for the HIV/AIDS epidemic, *Int. J. Biomath.*, **11**:1850086, 2018, https://doi.org/10.1142/S1793524518500869.
12. B. Kosko, Adaptive bi-directional associative memories, *Appl. Opt.*, **26**:4947–4960, 1987, https://doi.org/10.1364/AO.26.004947.
13. R. Kumar, S. Das, Y. Cao, Effects of infinite occurrence of hybrid impulses with quasi-synchronization of parameter mismatched neural networks, *Neural Netw.*, **122**:106–116, 2020, https://doi.org/10.1016/j.neunet.2019.10.007.
14. S. Lenhart, J.T. Workman, *Optimal Control Applied to Biological Models*, Chapman & Hall/CRC, Boca Raton, London, New York, 2007.
15. H. Li, J. Wang, P. Shi, Output-feedback based sliding mode control for fuzzy systems with actuator saturation, *IEEE Trans. Fuzzy Syst.*, **24**:1282–1293, 2016, https://doi.org/10.1109/TFUZZ.2015.2513085.

16. L. Li, C. Sun, J. Jia, Optimal control of a delayed SIRC epidemic model with saturated incidence rate, *Optim. Control. Appl. Metods*, **40**:367–374, 2019, https://doi.org/10.1002/oca.2482.

17. Y. Li, Y. Chen, I. Podlubny, Stability of fractional-order nonlinear dynamic systems: Lyapunov direct method and generalized Mittag–Leffler stability, *Comput. Math. Appl.*, **59**:1810–1821, 2010, https://doi.org/10.1016/j.camwa.2009.08.019.

18. B. Lundstrom, M. Higgs, W. Spain, A.L. Fairhall, Fractional differentiation by neocortical pyramidal neurons, *Nat. Neurosci.*, **11**:1335–1342, 2008, https://doi.org/10.1038/nn.2212.

19. C. Maharajan, R. Raja, J. Cao, G. Rajchakit, A. Alsaedi, Impulsive cohen-grossberg BAM neural networks with mixed time-delays: An exponential stability analysis issue, *Neurocomputing*, **275**:2588–2602, 2018, https://doi.org/10.1016/j.neucom.2017.11.028.

20. I. Podlubny, *Fractional Differential Equations*, Academic Press, San Diego, 1999.

21. L.S. Pontryagin, V.G. Boltyanskii, R.V. Gramkrelidze, E.F. Mishchenko, *The Mathematical Theory of Optimal Processes*, John Wiley & Sons, New York, 1962.

22. C. Pradeep, Y. Cao, R. Murugesu, R. Rakkiyappan, An event-triggered synchronization of semi-Markov jump neural networks with time-varying delays based on generalized free-weighting-matrix approach, *Math. Comput. Simul.*, **155**:41–56, 2019, https://doi.org/10.1016/j.matcom.2017.11.001.

23. P. Selvaraj, R. Sakthivel, O. M. Kwon, Synchronization of fractional-order complex dynamical network with random coupling delay, actuator faults and saturation, *Nonlinear Dyn.*, **94**:3101–3116, 2018, https://doi.org/10.1007/s11071-018-4516-3.

24. P. Selvaraj, R. Sakthivel, O.M. Kwon, Finite-time synchronization of stochastic coupled neural networks subject to Markovian switching and input saturation, *Neural Netw.*, **105**:154–165, 2018, https://doi.org/10.1016/j.neunet.2018.05.004.

25. O. Sharomi, T. Malik, Optimal control in epidemiology, *Ann. Oper. Res.*, **251**:55–71, 2017, https://doi.org/10.1007/s10479-015-1834-4.

26. I. Stamova, G. Stamov, Mittag–Leffler synchronization of fractional neural networks with time-varying delays and reaction-diffusion terms using impulsive and linear controllers, *Neural Netw.*, **96**:22–32, 2017, https://doi.org/10.1016/j.neunet.2017.08.009.

27. I. Stamova, G. Stamov, S. Simeonov, A. Ivanov, Mittag–Leffler stability of impulsive fractional-order bi-directional associative memory neural networks with time-varying delays, *Trans. Inst. Meas. Control*, **40**:3068–3077, 2017, https://doi.org/10.1177/0142331217714306.

28. T. Wang, J. Qiu, H. Gao, Adaptive neural control of stochastic nonlinear time-delay systems with multiple constraints, *IEEE Trans. Syst. Man Cybern. Part A Syst.*, **47**(8):1875–1883, 2017, https://doi.org/10.1109/TSMC.2016.2562511.

29. W. Wang, X. Wang, X. Luo, M. Yuan, Finite-time projective synchronization of memristor-based BAM neural networks and applications in image encryption, *IEEE Access*, **6**:56457–56476, 2018, https://doi.org/10.1109/ACCESS.2018.2872745.

30. Y. Wu, Z. Wu, H. Su, Synchronisation control of dynamical networks subject to variable sampling and actuators saturation, *IET Control Theory Appl.*, **9**:381–391, 2015, https://doi.org/10.1049/iet-cta.2014.0383.

31. J. Yan, J. Shen, Impulsive stabilization of impulsive functional differential equations by Lyapunov–Razumikhin functions, *Nonlinear Anal., Theory Methods Appl.*, **37**:245–255, 1999, https://doi.org/10.1016/S0362-546X(98)00045-5.

32. R. Ye, X. Liu, H. Zhang, J. Cao, Global Mittag–Leffler synchronization for fractional-order BAM neural networks with impulses and multiple variable delays via delayed-feedback control strategy, *Neural Process. Lett.*, **49**:1–18, 2018, https://doi.org/10.1007/s11063-018-9801-0.

33. M. Yuan, W. Wang, X. Luo, Asymptotic anti-synchronization of memristor-based BAM neural networks with probabilistic mixed time-varying delays and its application, *Mod. Phys. Lett. B*, **32**(24):1850287, 2018, https://doi.org/10.1142/S0217984918502871.

34. J. Zhang, J. Wu, H. Bao, J. Cao, Synchronization analysis of fractional-order three-neuron BAM neural networks with multiple time delays, *Appl. Math. Comput.*, **339**:441–450, 2018, https://doi.org/10.1016/j.amc.2018.06.013.

35. L. Zhang, Y. Yang, X. Xu, Synchronization analysis for fractional order memristive Cohen–Grossberg neural networks with state feedback and impulsive control, *Physica A*, **506**:644–660, 2018, https://doi.org/10.1016/j.physa.2018.04.088.